The EMBO Journal Vol. 21 No. 14 pp. 3569–3574, 2002

Projection structure at 8 Å resolution of the melibiose permease, an Na–sugar co-transporter from *Escherichia coli*

Ingrid Hacksell, Jean-Louis Rigaud[1], Pasi Purhonen, Thierry Pourcher[2], Hans Hebert[3] and Gérard Leblanc[2]

Karolinska Institutet, Department of Biosciences, S-141 57 Huddinge, Sweden, [1]Institut Curie, UMR-CNRS 168 and LRC-CEA 8, 11 rue Pierre et Marie Curie, 75231 Paris cedex 05 and [2]UMR 6078 CNRS-Université de Nice and LRC CEA 16, 06230 Villefranche-sur-mer, France

[3]Corresponding author
e-mail: Hans.Hebert@csb.ki.se

The ion-coupled sugar membrane symporter or co-transporter melibiose permease (MelB), responsible for α-galactoside accumulation in *Escherichia coli*, is a representative member of the glycoside–pentoside–hexuronide family of the vast class of electrochemical potential-driven porters. Pure solubilized preparations of a MelB recombinant protein were subjected to two-dimensional crystallization trials and several crystal forms were observed. Two of these appeared as large wide tubes suitable for analysis by electron crystallography. Flattened tubes on carbon support film, embedded in amorphous ice prior to electron cryomicroscopy, showed two-sided plane group symmetries $P12_1$ or $P222_1$, with unit cell dimensions a = 89.9 Å, b = 51.6 Å, γ = 91.9° and a = 188.9 Å, b = 48.8 Å, γ = 90°, respectively. The projection map from the $P222_1$ crystals at 8 Å resolution displayed an asymmetric protein unit consisting of two domains lining a central and curve-shaped cleft. Together, the MelB monomer could host the 12 predicted transmembrane α-helices. Overall, the MelB helix packing arrangement compared more favorably with that of the Na^+/H^+ antiporter NhaA than that of the oxalate antiporter.

Keywords: electron crystallography/membrane protein/Na–sugar co-transport/symporter

Introduction

More than 2500 identified membrane transporters from archaebacteria to mammals have been put together to compose the vast class of electrochemical potential-driven porters (Saier, 2000). Using functional and phylogenic criteria, a vast number of separate families of porters are currently distinguished. Although a large fraction of these families are unrelated, others are, and accordingly clustered into three distinct superfamilies. The predominant one, including the LacY permease from *Escherichia coli*, is the major facilitator superfamily (MFS). In spite of the diversity, the transporters share functional as well as structural features. Thus, they utilize carrier-mediated processes either to catalyze downhill movement of solutes along transmembrane electrochemical gradients (uniporters) or to exploit these gradients to promote uphill transport by tightly coupling the flows of ions and solutes in the same (symporters) or opposite direction (antiporters). It is believed that the majority of transporters from these families share a common basic structural feature with 12 transmembrane α-helices, a structural motif also found in many other transport systems including those within the ABC transporter superfamily.

Although a significant number of these secondary transporters have been studied in detail, little is known about their structure, and no atomic resolution map has yet been reported. So far, the best characterized member is the Na^+/H^+ antiporter from *E.coli* (NhaA, Na^+/H^+ antiporter family) for which a projection map at 4 Å resolution and a three-dimensional structure determination at 7 Å in-plane resolution have been derived by electron crystallography analysis of two-dimensional crystals (Williams *et al*., 1999; Williams, 2000). More recently, a projection map at 6 Å resolution from two-dimensional crystals of the oxalate antiporter (OxlT, super-MFS family) from *Oxalobacter formigenes* has been reported (Heymann *et al*., 2001). Finally, the lactose permease (LacY) of *E.coli*, also a member of the MFS superfamily, has been characterized extensively with several methods including two-dimensional crystallization (Zhuang *et al*., 1999), but no detailed structural information has been published so far.

In the present study, aiming for direct structural information, we made use of available procedures for large-scale purification to homogeneity of a recombinant, His-tagged, Na^+–sugar symporter (or co-transporter) melibiose permease (MelB) from *E.coli* (Pourcher *et al*., 1995). MelB, encoded by the *melB* gene (Yazyu *et al*., 1984), is a member of the glycoside–pentoside–hexuronide family, which is distinct from the MFS superfamily (Poolman *et al*., 1996; Paulsen *et al*., 2000). It is responsible for the co-transport of either Na^+, Li^+ or H^+ and the α-galactoside melibiose in *E.coli* (reviewed in Pourcher *et al*., 1990). MelB is a highly hydrophobic protein of 473 amino acid residues (M_r 52 kDa). A topological model that includes 12 hydrophobic transmembrane domains (TMs), with the N- and C-termini facing the cytoplasm, is predicted by hydropathy profiling of its primary amino acid sequence (Yazyu *et al*., 1984; Pourcher *et al*., 1993) and supported by MelB–alkaline phosphatase fusion analysis (Botfield *et al*., 1992; Pourcher *et al*., 1996) and proteolytic cleavage mapping (Gwizdek *et al*., 1997). High α-helical secondary structure content, possibly corresponding to transmembrane helices, has been detected by Fourier transform infrared spectroscopy (Dave *et al*., 2000).

Here we report on the successful production of two-dimensional crystals after reconstitution of purified MelB

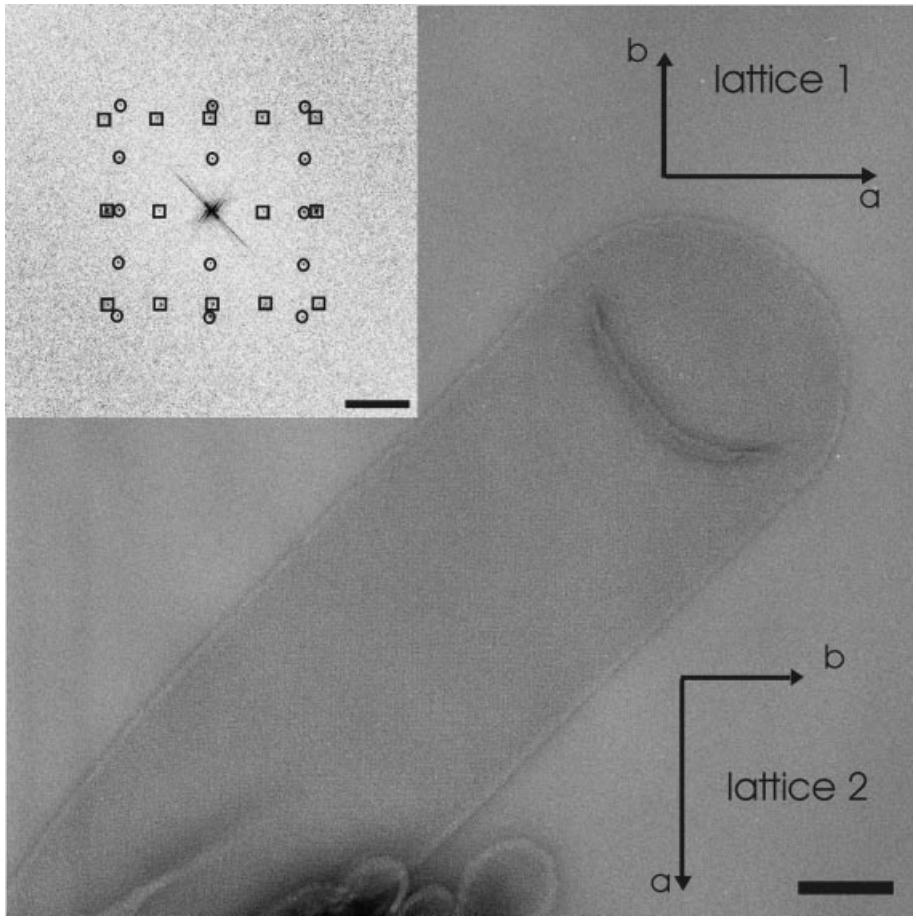

Fig. 1. Negatively stained tubular crystal of MelB of the $P12_1$ type showing the orientations of the lattices arising from the two sides of the tube following collapse on the carbon support film. The inset shows the corresponding diffraction pattern, with the spots from the two lattices marked with circles and squares, respectively. Scale bars: 100 nm (micrograph), 1/75 $Å^{-1}$ (diffraction pattern).

with *E.coli* lipids. The projection structure was determined at 8 Å resolution by cryoelectron microscopy and the map was compared with those previously reported for other 12 transmembrane helices transporters or proteins including NhaA and OxlT.

Results and discussion

Detergent removal from MelB–*E.coli* lipids–dodecyl maltoside (DDM) micellar solutions, either through a combination of Bio-Beads treatment and dialysis or by dialysis alone, resulted in the formation of two-dimensional crystals of MelB in the form of either single layers or flattened tubes. In general, the tubular crystals were larger and better ordered than the single layers and thus more suitable for structure analysis by electron crystallography. The tubes often had a width of 0.2–0.5 μm and extended up to several μm in length. Upon deposition on a continuous carbon film, the MelB tubes became flattened into two layers of well-preserved two-dimensional crystals. The two lattices appeared rotated by almost 90° relative to each other and with the unit cell axes at 45° relative to the long axis of the tube (Figure 1). The tubes, often protruding from large aggregates, were easily detected in the electron microscope at low magnification.

Membranes with a tubular shape always displayed protein molecules arranged into two-dimensional crystals with varying degree of order (Figure 2). Two different types of tubular crystals were observed with two-sided plane group symmetries $P12_1$ and $P222_1$, respectively (Table I). The calibrated unit cell parameters for the monoclinic type were $a = 89.9$ Å (SD 2.9, $n = 7$), $b = 51.6$ Å (SD 1.4, $n = 7$), $\gamma = 91.9°$ (SD 1.2, $n = 7$), while the orthorhombic form measured $a = 188.9$ Å (SD 2.1, $n = 26$), $b = 48.8$ Å (SD 0.6, $n = 26$), $\gamma = 90°$. Assuming that two protein molecules of MelB occupied the small unit cell and four were present in the larger, the packing densities were very similar, 22.4 and 22.6 $Da/Å^2$, respectively. These values are lower than the molecular packing in other highly hydrophobic proteins with most of their molecular mass in the phospholipid bilayer, such as bacteriorhodopsin (25.1 $Da/Å^2$), aquaporin (24.8 $Da/Å^2$), MIP (27.6 $Da/Å^2$) and microsomal glutathione transferase (24.9 $Da/Å^2$).

Analysis of unstained specimens was carried out for the $P222_1$ crystal form, which was the more abundant in the reconstituted preparations. The projection structure is consistent with four protein molecules occupying the unit cell (Figure 3). It is noteworthy that the 2-fold rotation axes perpendicular to the plane of the membrane and intersecting the long unit cell axis relate two protein units

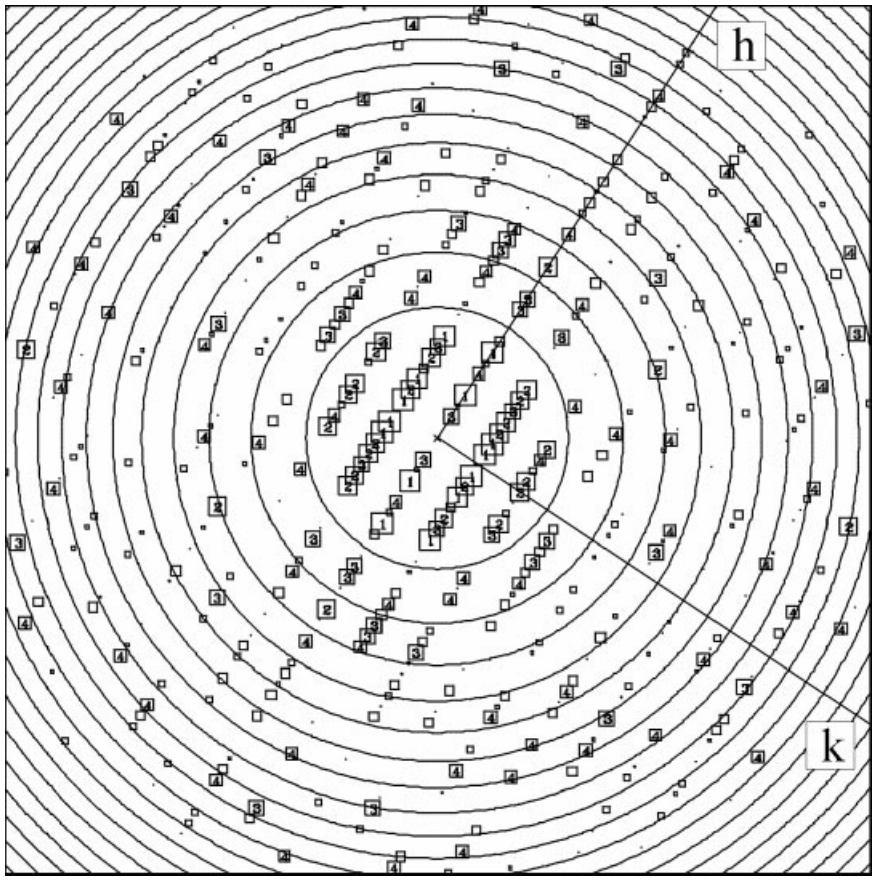

Fig. 2. Calculated Fourier transform amplitudes from a MelB crystal after unbending. The size of the squares and the numbers correspond to the IQ value of the spots (Henderson *et al*., 1986). The rings depict the positions of the zero crossings of the contrast transfer function at the defocus value of 10 100 Å. The half-width of the box corresponds to spatial frequency 1/5.6 $Å^{-1}$.

Table I. Electron crystallographic data

Two-sided plane group symmetry[a]		$P222_1$	
Unit cell parameters, Å		a = 188.9 (SD 2.1, n = 26)	
		b = 48.8 (SD 0.6, n = 26)	
		γ = 90°	
No. of crystals used for merging		6	
No. of observations, IQ⩽7		491	
No. of unique observations		101	
Overall phase residual[b] to 8 Å, IQ⩽5		30.0°	
Phase residual (no. of observations)[c]	200–20 Å	26.7° (27)	35.5° (18)
	20–15 Å	28.0° (17)	39.6° (7)
	15–10 Å	32.0° (22)	46.6° (8)
	10–8 Å	33.3° (24)	37.7° (9)
Overall phase error during merging[d]		36.7°	
B-factor for final map calculation		350	

[a]Determined using ALLSPACE (Valpuesta *et al*., 1994). For example, the data from crystal 7472 gave a phase residual of 39.0° for 130 comparisons in $P222_1$, to be compared with the target residual of 36.4.
[b]Averaged phase deviations from 0° or 180° for the vectorially averaged phases based on observations from the six individual crystals.
[c]Within each resolution range, two values are given. The first one is the deviation from 0° or 180° (random value 45°) while the second was obtained by splitting the data set into two halves and comparing spots with the same indices and observed in both sets (random 90°).
[d]Averaged agreement of phase values between observations from the individual crystals.

that are close together. The interaction surface between the two protein units about the 2-fold rotation axes is limited to one of the tips of the molecule. The contact surfaces at the positions of the in-plane 2-fold rotations are between adjacent protein units in up and down orientations relative to the membrane plane. This crystal organization is different from those reported for the NhaA and OxlT transporters, respectively. In reconstituted two-dimensional crystals, these last two 12 TM transporters have been shown to occur also as dimers, but to be present in alternately up and down orientations. These data, together with our MelB projection map, tend to suggest that

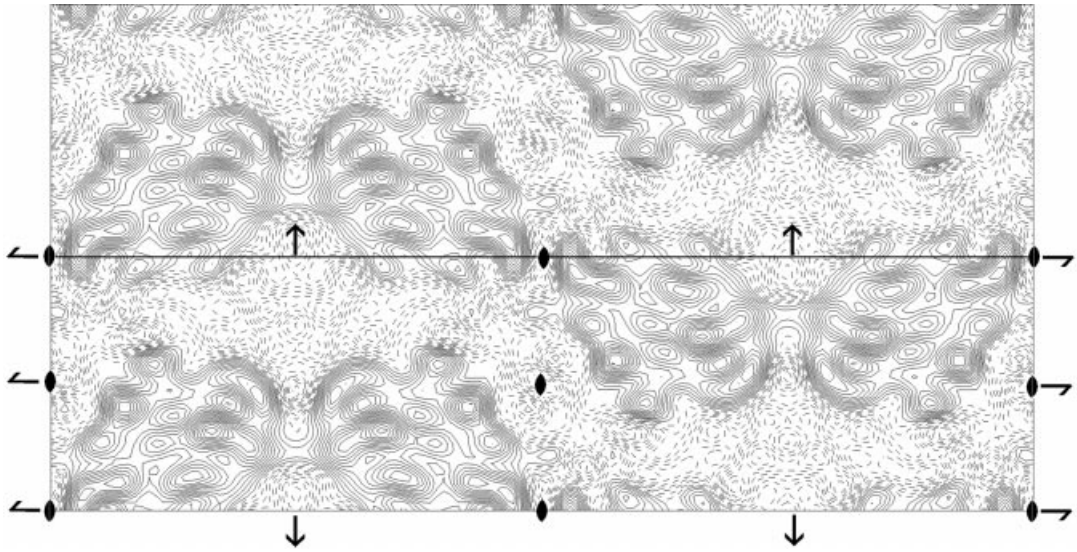

Fig. 3. Projection map at 8 Å resolution of MelB $P222_1$ two-dimensional crystals embedded in vitreous ice prior to electron microscopy. The map was calculated from merged amplitudes and phases from six independent lattices. The amplitude and phase relationships of the two-sided plane group were applied. The 2-fold rotation axes perpendicular to the plane of the membrane and the 2-fold rotation axes and the 2-fold screw axes in the membrane plane are depicted in one of the two unit cells shown. The in-plane 2-fold rotation is parallel to the short 48.8 Å axis of the unit cell, while the 2-fold screw is along the direction of the 188.9 Å unit cell axis. Solid contour lines indicate density above the mean, while density below the mean is depicted by dashed lines. The contour levels were drawn at density levels corresponding to 0.2 of the r.m.s. value of the map. The r.m.s. value was 0.24 of the maximum density. Four symmetry-related protein-dense regions are observed in each unit cell corresponding to the projections of the MelB molecules.

protein–protein interactions in all two-dimensional crystals of these transporters reflect favorable crystallographic interactions rather than *in vivo* protein contacts.

Each monomer of MelB had a size of ~49 Å × 37 Å (Figure 3). It is worth noting that the size of the MelB monomer compares well with that computed from the electron microscopic projection maps of both the NhaA transporter (48 × 38 Å^2) (Williams *et al*., 1999) and the OxlT transporter (48 × 32 Å^2) (Heymann *et al*., 2001). Comparatively, the area of the multidrug transporter EmrE molecules, with only eight helices per monomer, is smaller (31 × 40 Å^2; Tate *et al*., 2001). Evidence from these studies together with information on the three-dimensional structural organization of NhaA (Williams, 2000) support the notion that 12 TM helices may well be fitted within the projection area of the MelB monomer.

Although assignment of dense areas to individual transmembrane α-helices is by no means conclusive when dealing with limited resolution projection maps, previous studies on other membrane proteins (e.g. bacteriorhodopsin and NhaA) demonstrated that it is often of good predictive value. Accordingly, we tentatively assigned discrete dense areas with varying intensity level and shape in the projection map (arbitrarily labeled from A to L) to the 12 TM helices of MelB (Figure 4). The four best resolved density peaks (A, B, C and J) can be assigned to TM helices oriented nearly perpendicular with respect to the membrane plane. Five other densities (D, E, F, H and L), displaying more or less elongated projected areas, may well predict the presence of tilted α-helices. The three remaining poorly resolved dense areas termed G, I and K may also result from the projection of tilted helices. These predictions would suggest that about two-thirds of the MelB helices have significant degrees of

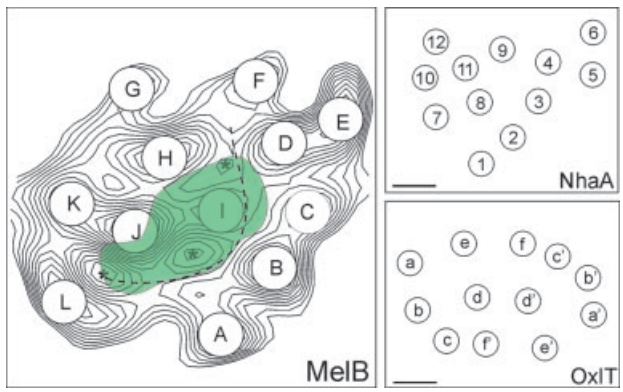

Fig. 4. One molecule of MelB together with positions and indexing of α-helices in the Na^+/H^+ antiporter NhaA (Williams *et al*., 2000) and the oxalate transporter OxlT (Heymann *et al*., 2001). Protein-dense regions in the MelB map have been marked with letters (A–L). Asterisks indicate internal density minima in the structure. The dashed line shows protein-deficient regions dividing the projection structure into two parts. A possible aqueous channel corresponds to the elongated green domain enclosing the inner protein-deficient regions in the projection map. The boxed area corresponds to one-quarter of the unit cell, with the horizontal dimension equal to one-quarter of the unit cell parameter a = 47.2 Å and the vertical dimension equal to the length of the b-axis, 48.8 Å. The scale bars for NhaA and OxlT correspond to 10 Å.

inclination angles with respect to the normal of the membrane plane. Direct or indirect evidence for a significant proportion of tilted α-helices in most membrane proteins including pumps, secondary or ABC transporters is abundant. Of direct interest for the comparison of the structure of other transporters from the same class of electrochemical potential-driven porters is the observation by Williams (2000) that most NhaA α-helices are tilted substantially (10–27°). From the

projection map of OxlT, five α-helices are interpreted as closely aligned to the membrane normal, while the remaining seven could be tilted or kinked (Heymann *et al*., 2001). The resolution of our projection map is not sufficient to interpret any of the densities as arising from re-entrant loops such as those actually observed in aquaporin (Murata *et al*., 2000) or those suggested to be present in bacterial transporters, neurotransmitter transporters and ion exchanger antiporters (Slotboom *et al*., 1999; Wakabayashi *et al*., 2000). Finally, the projection map shows three internal areas of lower density (marked with asterisks in Figure 4). It could be noted that, all together, these three lower densities might correspond to a central curve-shaped cleft as in the projection map of OxlT.

Another interesting characteristic of the projected MelB structure is the clear observation that the 12 dense areas are distributed asymmetrically within two regions (Figure 4). These two domains are distinguished more easily by considering their position relative to the central, curve-shaped cleft that could be assimilated to a putative intraprotein aqueous co-substrate pathway. The region bordering the right-hand side of the cleft is elongated and forms an arc composed of six mostly peripheral densities (A–F). The other domain lining the left-hand boundaries of the cleft includes the six remaining densities (G–L) organized into a more compact and roughly triangular bundle with its apex pointing towards the cleft. Two peak densities (I and J) of this compact bundle are clearly located within the core of the protein and thus not in contact with outer lipids. Both the asymmetric density arrangement and shape of the two regions of MelB are similar to what has been reported for the NhaA antiporter structure (Williams *et al*., 1999; Williams, 2000; Figure 4), although the asymmetric arrangement in NhaA could have been related to an inactive conformational state of NhaA under the very acidic condition (pH 4.0) used for its crystallization. No such restriction exists in interpreting the MelB map structure as the purified Na-coupled symporter retains full binding activity and function in the milder acidic (pH 6.0) conditions used for crystallization (see Pourcher *et al*., 1990, 1995). The OxlT structure differs radically from that of MelB and NhaA, as a quasi 2-fold symmetry was observed between two six-helical bundles (Heymann *et al*., 2001; Figure 4). The authors pointed out that such symmetry could possibly be related to the homology detected by sequence analysis between the first six and the last six helices and associated with ancient gene duplication. This feature is common to members of porter families merged into the MFS superfamily. Evidence for such gene duplication in Na-coupled porters and MelB is much weaker (Reizer *et al*., 1994; Williams *et al*., 1999). This comparison suggests that the helix packing organization of unrelated electrochemical potential-driven transporters may differ from one family or superfamily to the other.

While awaiting higher resolution, an interesting working hypothesis for the asymmetry of MelB and NhaA can be raised in light of their shared high specificity towards Na^+ ions. Several mutagenesis studies on MelB (reviewed in Poolman *et al*., 1996) or on NhaA (reviewed in Padan, 2001) have led to the suggestion that acidic residues (mainly located in N-terminal helices I, II or IV) are involved in the process of Na^+ recognition. For MelB, it has been suggested that the acidic residues might cooperate by forming a coordination network for Na^+, Li^+ or hydronium, but not for K^+ ions (Pourcher *et al*., 1993). The strict structural constraints imposed by the relative position of the coordination ligands and implicit tight packing of the helices supporting them would predict the existence of at least one subdomain of higher density in the projection map of an Na-coupled symporter or antiporter. In the case of MelB, the dense subdomain might well account for the presence of the more compact and roughly triangular bundle comprising the H, I and J densities observed in the projection map. The frequent conservation of N-terminal regions in many (but not all) families of Na–solute symporters (Reizer *et al*., 1994) would favor the idea that this structural feature is shared by other Na-coupled porters. Finally, it is worth noting that recent topological information derived from cysteine scan mutagenesis, accessibility to impermeant SH reagent studies or second-site revertant analyses also provides support for the presence of an asymmetric arrangement of MelB helices and of a dense subregion in the molecule structure (Ding and Wilson, 2001). In the resulting topological model, helices TM1–TM4 are clustered into a compact bundle on one side of the molecule, which is separated from a curve-shaped region comprising several C-terminal helices by the aqueous substrate pathway of the transporter.

In conclusion, the present study describes the first successful crystallization of an Na^+-dependent symporter or co-transporter at a resolution that provides significant structural information. The information derived from the projection map of MelB at 8 Å resolution strongly suggests that MelB's structure has an asymmetric organization. This conclusion is strengthened by concordant prediction from structural and topological studies. Taking into account that the NhaA antiporter structure also has an asymmetrical organization, we suggest that this motif is a possible signature of Na-dependent porters included in different families of the vast class of electrochemical potential-driven porters.

Materials and methods

MelB carrying a His_6 tag at its C-terminal extremity (MelB-6His) was purified to homogeneity by affinity chromatography in 0.1% DDM and at a final concentration of 1 mg/ml as described by Pourcher *et al*. (1995). Sample purity was better than 99% as judged by SDS–PAGE and silver staining and by gel filtration. Na-dependent binding measurements of a high affinity sugar analog indicated that, in the interval of pH 6–8, at least 80% of the MelB-6His in the samples to be used for crystallization trials were active.

For two-dimensional crystallization experiments, the protein was kept at a concentration of ~1 mg/ml in a buffer containing 20 mM Tris–HCl pH 8, 50 mM NaCl, 5 mM melibiose, 5 mM 2-mercaptoethanol, 10% glycerol, 0.1% DDM and 100 mM imidazole. The protein was incubated for 1 h with *E.coli* lipids (Avanti Polar Lipids, Alabaster, AL). Lipids were added as liposome suspensions pre-treated with a saturating amount of DDM or octyl-β-glucoside. The molar lipid to protein ratio was varied between 25 and 40. The mixture was dialyzed against detergent-free citric buffer, 20 mM, at pH 6, containing 200 mM NaCl, 5 mM melibiose, 5 mM 2-mercaptoethanol and 10% glycerol for 9 days either with or without pre-treatment with Bio-Beads SM2 (Bio-Rad, Hercules, CA) for 1 h. The crystallization was performed at 22°C and the crystals were stable upon storage at 4°C for several weeks.

The crystallization experiments were evaluated by electron microscopy following negative staining in 1% uranyl acetate. A Philips CM120

electron microscope (FEI, Eindhoven, The Netherlands) run at 120 kV and equipped with a Tietz CCD camera (TVIPS GmbH, Gauting, Germany) was used. Successful crystallization attempts were analyzed further by low dose electron cryomicroscopy using the same equipment but with recordings at a nominal magnification of 60 000× on Kodak SO-163 film. The micrographs were developed in concentrated D-19 developer for 12 min. The specimens were either embedded in glucose or tannin (Wang and Kühlbrandt, 1991) by the back injection method (Hirai *et al*., 1999) or frozen in liquid ethane and subsequently transferred to a cryo holder (Gatan Inc. Pleasanton, CA) cooled by liquid nitrogen to a temperature of approximately –175°C. Optical diffraction was used to evaluate the quality of the crystals and the micrographs. Selected images were subjected to densitometry using a Zeiss SCAI scanner set at 7 μm pixel size, corresponding to 1.14 Å on the specimen level as determined through calibration of the electron optical magnification by simultaneous observations of two-dimensional crystals of microsomal glutathione transferase for which the unit cell parameters are known accurately (Hebert *et al*., 1997).

Image processing was performed using the MRC program suite (Crowther *et al*., 1996) run on DEC Alpha workstations. Basically, the crystals, scanned into 6000 × 6000 pixel squares, were adjusted for lattice distortions (Henderson *et al*., 1986) following indexing of the two different lattices arising from the two sides of the collapsed tubular crystals. Extracted amplitudes and phases were corrected for the contrast transfer function at typical underfocus values of 4000–10 000 Å. The symmetries of the two predominant crystal forms were determined by running several data sets through ALLSPACE (Valpuesta *et al*., 1994). Data from six crystals were merged and projection maps calculated using CCP4 programs (CCP4, 1994).

Acknowledgements

The authors are particularly indebted to Raymonde Lemonnier (Villefranche sur mer) for her technical skill in the preparation of the purified MelB samples. This project was supported by grants from the European Commission (G.L., J.L.R. and H.H., contract BIO4-CT-972119), the Atomic Energy Commission and CNRS (G.L. and J.L.R.) and the Swedish Research Council (H.H.). A long-term fellowship from the Graduate School of Electron Microscopy and Structural Characterization, Tampere, Finland is gratefully acknowledged (P.P.).

References

Botfield,M.C., Naguchi,K., Tsuchiya,T. and Wilson,T.H. (1992) Membrane topology for the melibiose carrier of *Escherichia coli*. *J. Biol. Chem.*, **267**, 1818–1822.

CCP4 (1994) The CCP4 suite: programs for protein crystallography. *Acta Crystallogr. D*, **50**, 760–763.

Crowther,R.A., Henderson,R. and Smith,J.M. (1996) MRC image processing programs. *J. Struct. Biol.*, **116**, 9–16.

Dave,N., Troullier,A., Mus-Veteau,I., Dunach,M., Leblanc,G. and Padros,E. (2000) Secondary structure components and properties of the melibiose permease from *Escherichia coli*: a Fourier transform infrared spectroscopy analysis. *Biophys. J.*, **79**, 747–755.

Ding,P.Z. and Wilson,T.H. (2001) Cysteine mutagenesis of the amino acid residues of transmembrane helix I in the melibiose carrier of *Escherichia coli*. *Biochemistry*, **40**, 5506–5510.

Gwizdek,C., Leblanc,G. and Bassilana,M. (1997) Proteolytic mapping and substrate protection of the *Escherichia coli* melibiose permease. *Biochemistry*, **36**, 8522–8529.

Hebert,H., Schmidt-Krey,I., Morgenstern,R., Murata,K., Hirai,T., Mitsuoka,K. and Fujiyoshi,Y. (1997) The 3.0 Å projection structure of microsomal glutathione transferase as determined by electron crystallography of $p2_12_12$ two-dimensional crystals. *J. Mol. Biol.*, **271**, 751–758.

Henderson,R., Baldwin,J.M., Downing,K.H., Lepault,J. and Zemlin,F. (1986) Structure of purple membrane from *Halobacterium halobium*: recording, measurement and evaluation of electron micrographs at 3.5 Å resolution. *Ultramicroscopy*, **19**, 147–178.

Heymann,J.A.W., Sarker,R., Hirai,T., Shi,D., Milne,J.L.S., Maloney, P.C. and Subramaniam,S. (2001) Projection structure and molecular architecture of OxlT, a bacterial membrane transporter. *EMBO J.*, **20**, 4408–4413.

Hirai,T., Murata,K., Mitsuoka,K., Kimura,Y. and Fujiyoshi,Y. (1999) Trehalose embedding technique for high-resolution electron crystallography: application to structural study on bacterial rhodopsin. *J. Electron Microsc.*, **48**, 653–658.

Murata,K., Mitsuoka,K., Hirai,T., Walz,T., Agre,P., Heymann,J.B., Engel,A. and Fujiyoshi,Y. (2000) Structural determinants of water permeation through aquaporin-1. *Nature*, **407**, 599–605.

Padan,E., Venturi,M., Gerchman,Y. and Dover,N. (2001) Na^+/H^+ antiporters. *Biochim. Biophys. Acta*, **1505**, 144–157.

Paulsen,I.T., Nguyen,L., Sliwinski,M.K., Rabus,R. and Saier,M.H.,Jr (2000) Microbial genome analyses: comparative transport capabilities in eighteen prokaryotes. *J. Mol. Biol.*, **301**, 75–100.

Poolman,B., Knol,J., van der Does,C., Henderson,P.J., Liang,W.J., Leblanc,G., Pourcher,T. and Mus-Veteau,I. (1996) Cation and sugar selectivity determinants in a novel family of transport proteins. *Mol. Microbiol.*, **19**, 911–922.

Pourcher,T., Bassilana,M., Sarkar,H.K., Kaback,H.R. and Leblanc,G. (1990) The melibiose/Na^+ symporter of *Escherichia coli*: kinetic and molecular properties. *Philos. Trans. R. Soc. Lond., B Biol. Sci.*, **326**, 411–423.

Pourcher,T., Zani,M.L. and Leblanc,G. (1993) Mutagenesis of acidic residues in putative membrane-spanning segments of the melibiose permease of *Escherichia coli*. I. Effect on Na^+-dependent transport and binding properties. *J. Biol. Chem.*, **268**, 3209–3215.

Pourcher,T., Leclercq,S., Brandolin,G. and Leblanc,G. (1995) Melibiose permease of *E.coli*: large scale purification and evidence that H^+, Na^+ and Li^+ sugar symport is catalyzed by a single polypeptide. *Biochemistry*, **34**, 4412–4420.

Pourcher,T., Bibi,E., Kaback,H.R. and Leblanc,G. (1996) Membrane topology of the melibiose permease of *Escherichia coli* studied by *melB–phoA* fusion analysis. *Biochemistry*, **35**, 4161–4168.

Reizer,J., Reizer,A. and Saier,M.H.,Jr (1994) A functional superfamily of sodium/solute symporters. *Biochim. Biophys. Acta*, **1197**, 133–166.

Saier,M.H.,Jr (2000) A functional–phylogenetic classification system for transmembrane solute transporters. *Microbiol. Mol. Biol. Rev.*, **64**, 354–411.

Slotboom,D.J., Sobczak,I., Konings,W.N. and Lolkema,J.S. (1999) A conserved serine-rich stretch in the glutamate transporter family forms a substrate-sensitive reentrant loop. *Proc. Natl Acad. Sci. USA*, **96**, 14282–14287.

Tate,C.G., Kunji,E.R.S., Lebendiker,M. and Schuldiner,S. (2001) The projection structure of EmrE, a proton-linked multidrug transporter from *Eschericia coli* at 7 Å resolution. *EMBO J.*, **20**, 77–81.

Valpuesta,J.M., Carrascosa,J.L. and Henderson,R. (1994) Analysis of electron microscope images and electron diffraction patterns of thin crystals of ϕ29 connectors in ice. *J. Mol. Biol.*, **240**, 281–287.

Wakabayashi,S., Pang,T., Su,X. and Shigekawa,M. (2000) A novel topology model of the human Na^+/H^+ exchanger isoform 1. *J. Biol. Chem.*, **275**, 7942–7949.

Wang,D.N. and Kühlbrandt,W. (1991) High-resolution electron crystallography of light-harvesting chlorophyll *a/b*-protein complex in three different media. *J. Mol. Biol.*, **217**, 691–699.

Williams,K.A. (2000) Three-dimensional structure of the ion-coupled transport protein NhaA. *Nature*, **403**, 112–115.

Williams,K.A., Geldmacher-Kaufer,U., Padan,E., Schuldiner,S. and Kühlbrandt,W. (1999) Projection structure of NhaA, a secondary transporter from *Escherichia coli*, at 4.0 Å resolution. *EMBO J.*, **18**, 3558–3563.

Yazyu,H., Shiota-Niiya,S., Shimamoto,T., Kanazawa,H., Futai,M. and Tsuchiya,T. (1984) Nucleotide sequence of the *melB* gene and characteristics of deduced amino acid sequence of the melibiose carrier of *Escherichia coli*. *J. Biol. Chem.*, **259**, 4320–4326.

Zhuang,J., Privé,G.G., Werner,G.E., Ringler,P., Kaback,H.R. and Engel,A. (1999) Two-dimensional crystallization of *Escherichia coli* lactose permease. *J. Struct. Biol.*, **125**, 63–75.

Received February 22, 2002; revised and accepted May 24, 2002